UNIVERSIDAD COMPLUTENSE DE MADRID

FACULTAD DE CIENCIAS FÍSICAS

DEPARTAMENTO DE FÍSICA TEÓRICA

TRABAJO DE FIN DE GRADO

Código TFG: FT03

Agujeros negros en gravedad semiclásica

Black holes in semiclassical gravity

Supervisores: Luis J. Garay, Álvaro Álvarez Domínguez

Joaquín Gabriel Márquez Olguín

Grado en Física

Curso académico 2024-25

Convocatoria 2025

Calificación: 9.6

Agujeros negros cargados en gravedad semiclásica

Resumen:

En la ausencia de una teoría cuántica de la gravedad, la gravedad semiclasica ha demostrado ser un marco teórico fructífero en el que se trata al espaciotiempo como un fondo clásico fijo, mientras que los campos de materia y energía se cuantizan. En este trabajo, comenzamos construyendo las extensiones analíticas máximas de los espaciotiempos de Rindler, Schwarzschild y Reissner-Nordström, y analizamos sus estructuras causales mediante diagramas de Penrose. A continuación, estudiamos la dinámica de un campo escalar cargado en un espaciotiempo curvo genérico a través de la cuantización canónica, centrándonos en la ambigüedad que surge al definir los estados de vacío en diferentes esquemas de cuantización, y en cómo esta ambigüedad da lugar a un contenido de partículas dependiente del observador, formalizado mediante el uso del transformaciones de Bogoliubov. Finalmente, exploramos la superradiancia de carga: un proceso en el que ondas cargadas son amplificadas al dispersarse en el fondo de un agujero negro cargado. A nivel clásico, derivamos el régimen de frecuencias en el que ocurre este efecto, y mostramos que, en ese mismo régimen, su análogo cuántico conduce a un flujo no nulo de partículas en el estado de vacío 'in'—vacío de partículas en el infinito nulo pasado—con respecto al estado de vacío 'out'—vacío de partículas en el infinito nulo futuro.

Abstract:

In the absence of a quantum theory of gravity, semiclassical gravity represents a fruitful theoretical framework where spacetime is treated as a fixed classical background and matter and energy fields are quantized. In this thesis, we begin by constructing the maximal analytic extensions of Rindler, Schwarzschild, and Reissner-Nordström spacetimes, analyzing their causal structures using Penrose diagrams. We then study the dynamics of a charged scalar field in a generic curved spacetime through canonical quantization, focusing on the ambiguity in defining vacuum states between different quantization schemes and how they lead to observer-dependent particle content using the Bogoliubov formalism. Finally, we explore charge superradiance: a process in which charged waves are amplified when scattered from a charged black hole background. Classically, we derive the frequency regime where this effect occurs, and show that in the same regime its quantum analogue leads to a non-zero flux of particles in the vacuum state 'in'—which is devoid of particles at past null infinity—with respect to the vacuum state 'out'—which is devoid of particles at future null infinity.

Contents

1 Introduction

Reconciling general relativity and quantum mechanics into a unified theory remains one of the deepest challenges in modern physics. On the one hand, general relativity offers a unique geometric description of gravity: matter tells spacetime how to curve, and curved spacetime tells matter how to move [1]. This classical theory has proven to accurately predict the behavior of massive objects and the dynamics of the universe on large scales. Quantum field theory (QFT), on the other hand, successfully explains the physics behind fundamental particles and their interactions at the smallest scales [2].

However, these two pillars of physics are built on conceptually incompatible principles. General relativity is a deterministic, geometric theory of a dynamical spacetime, while QFT is a probabilistic framework where particles emerge as excitations of quantum fields defined on a fixed spacetime background. Because of this, combining them into a full theory of quantum gravity has proven extremely challenging up to date. In the absence of such a theory, semiclassical gravity serves as an intermediate step, in which spacetime is treated as a fixed classical background, while matter fields are quantized and evolve according to the principles of QFT.

Despite its limitations—such as neglecting the backreaction of matter on the geometry—this approximation framework has provided some interesting results, especially related to black hole physics. Probably the most striking one is Hawking radiation [3]: when considering quantum fields on the background of an evaporating black hole, particles are spontaneously emitted as thermal radiation due to fluctuations in the quantum vacuum.

To better understand such black hole phenomena, one must first carefully analyze the geometry of their spacetimes. An important aspect in general relativity is the appearance of singularities in some solutions to Einstein's equations. However, not all singularities reflect a true physical breakdown of the spacetime manifold. Some of them are known as 'coordinate' singularities: mere artifacts that arise due to a poor choice of coordinates and can be removed via a suitable coordinate transformation, allowing us to extend the geometry further. Therefore, distinguishing between truly physical and coordinate-related singularities is a necessary step to understand the causal structure of black hole spacetimes. We will explore these distinctions by studying the maximal analytical extension of several spacetimes using tools such as Penrose diagrams [4].

At the same time, when quantum fields are introduced on these curved backgrounds, another rather subtle issue arises: how to define what we mean by 'particles'. In flat Minkowski spacetime, Poincaré invariance allow us to uniquely define modes with positive and negative norm—with respect to a given inner product—for scalar fields [5]. These, in turn, define a preferred vacuum state—a state annihilated by all annihilation operators—and hence a well-defined notion of particles and antiparticles. But this is no longer the case in curved spacetime, where there is generally no preferred criterion. As a result, the splitting of mode solutions becomes ambiguous: different observers can disagree on whether a given mode represents a particle, an antiparticle, or even the vacuum itself.

One of the key conceptual questions addressed in this thesis is how to define the splitting of the mode solutions into positive and negative norm components. In order to do so, one introduces the Klein-Gordon (KG) product [6]. This product—which allows us to talk about the orthogonality and normalization of scalar field modes—is not positive definite, meaning that it can yield positive and negative values. This key property enables us to distinguish between particles—associated with modes with positive KG norm—and antiparticles—associated with those with negative KG norm. As a consequence, the notion of particles and antiparticles becomes dependent on the chosen basis of modes, which in turn determines the sets of annihilation and creation operators used to build the corresponding Fock spaces. Then, different choices of basis might lead to different quantization schemes and vacuum states. One way we have to compare them is by means of

Bogoliubov transformations, which relate two sets of basis solutions and quantify how much of the 'particle content' of one vacuum is seen by another. In particular, we will see that when the Bogoliubov β-coefficients are non-zero, there is a mixing between modes of positive and negative KG norm, and therefore also between the notions of particles and antiparticles from the two quantization schemes. This underlines the ambiguity in the definition of quantum vacuum and is the origin of phenomena such as the Unruh effect [7].

A particular manifestation of this vacuum ambiguity which we will study is 'charge superradiance' [8], a quantum analogue of a classical effect where charged bosonic waves get amplified after being scaterred off a charged black hole. Classically, it is observed that the incident charged scalar fields have a reflection coefficient larger than one in a specific range of frequencies—the so-called superradiant regime. This effect possesses a quantum counterpart in which certain vacuum states can exhibit a non-vanishing flux of outgoing particles, which comes from the mismatch between the so-called 'in' and 'out' quantum vacuum states, defined as those devoid of particles and antiparticles at future and past null infinities, respectively.

This thesis aims to introduce semiclassical gravity through the canonical quantization of a charged field in a curved, electromagnetic background, and discuss the phenomenon of charge superradiance which arises from the ambiguity in the choice of quantum vacuum. In Section 2, we begin by studying the causal structure and maximal analytical extension of several spacetimes: Rindler, Schwarzschild, and Reissner-Nordström. In Section 3, we formulate the canonical quantization of a charged scalar field in a general curved spacetime, introducing the KG product and Bogoliubov transformations as essential tools for comparing different quantum vacua. Finally, in Section 4 we explore the classical and quantum versions of charge superradiance in the Reissner-Nordström black hole background.

Throughout our analysis, we will use the metric signature $(-,+,+,+)$, and natural units with $c = G = 1$.

2 Classical background

Let us start by setting up the 'stage'—that is, the classical background—by analyzing the maximal analytical extension of different curved spacetimes: Rindler, Schwarzschild, and Reissner-Nordström. We pay special attention to distinguishing between physical and coordinate singularities, and how to represent the causal structure through Penrose diagrams.

2.1 Rindler metric

The Rindler metric [9] describes a portion of flat Minkowski spacetime as seen by uniformly accelerated observers. It can be obtained via a coordinate transformation from inertial Minkowski coordinates to a non-inertial frame undergoing constant proper acceleration κ. In 1+1 dimensions, it is given by

$$ds^2 = -(\kappa r)^2 dt^2 + dr^2, \tag{2.1}$$

for $t \in (-\infty, \infty)$ and $r \in (0, \infty)$.

At $r = 0$, the metric becomes degenerate and non-invertible, indicating the presence of a singularity. However, when curvature invariants like the Kretschmann scalar $R_{\mu\nu\rho\sigma}R^{\mu\nu\rho\sigma}$ are computed, no signs of a physical singularity arise at this point. It is crucial then to distinguish between true physical singularities—arising from the spacetime geometry itself—and 'coordinate singularities"—artifacts of the chosen coordinate system, which may fail to fully cover the entire spacetime manifold.

To determine what kind of singularity is present at $r = 0$, we can transition to a more suitable coordinate system: if the metric, when expressed in affine coordinates, still presents issues at the suspected singularity, it would imply geodesic incompleteness and we can confidently conclude that it is a real singularity; otherwise, it is a coordinate singularity that can be easily avoided via a coordinate transformation.

The metric can be rewritten as:

$$ds^2 = f(r)\left[-dt^2 + dr_*^2\right], \quad \text{where} \quad f(r) = (\kappa r)^2, \tag{2.2}$$

and we have introduced the 'tortoise' coordinate r_* defined by $dr_* = dr/(\kappa r)$, implying that $r_* = \kappa^{-1}\log(\kappa r)$ with range $r_* \in (-\infty, \infty)$. Despite this change of coordinates, the metric still presents the same issues at $r = 0$, where $r_* \to -\infty$. However, this new form of the metric shows that it is simply a conformal factor $f(r)$ multiplied by the Minkowski metric. This suggests that adopting null coordinates in two dimensions may be advantageous for several reasons: they simplify computations, separate incoming and outgoing geodesics, and allow for a clearer geometric interpretation of light cones. Additionally, in null coordinates, the propagation of light rays follows 45-degree lines, and their explicit form is well known for the case of Minkowski space, making them an ideal choice in this context [1].

The null coordinates are defined as

$$u = t - r_*, \quad v = t + r_*, \tag{2.3}$$

with $u, v \in (-\infty, +\infty)$. Expressing now the radial coordinate r in terms of these null coordinates allows us to rewrite the metric as

$$ds^2 = -e^{\kappa(v-u)} du\, dv = -dU\, dV, \tag{2.4}$$

where we have defined the Kruskal coordinates

$$U = -\kappa^{-1}e^{-\kappa u}, \quad V = \kappa^{-1}e^{\kappa v}. \tag{2.5}$$

It is important to note that while $u, v \in (-\infty, +\infty)$, the new coordinates $U \in (-\infty, 0)$ and $V \in (0, +\infty)$. Given the analytical expressions for U and V, it seems natural to extend them to range from $-\infty$ to $+\infty$, achieving what is known as the maximal analytic extension of the spacetime. Comparing it with the Minkowski spacetime metric in null coordinates, we see that they both cover the whole spacetime in the same way. Therefore, given that the coordinates U and V are affine, we conclude that the singularity we encountered at $r = 0$—that is, at $U = 0$ or $V = 0$—is not a physical singularity but a 'coordinate' one.

2.2 Schwarzschild metric

The Schwarzschild metric represents a spherically symmetric, static solution to the vacuum Einstein field equations, $R_{\mu\nu} - \frac{1}{2}g_{\mu\nu}R = 0$, and describes the spacetime geometry surrounding a non-rotating, uncharged massive object. The line element of this solution is given by

$$ds^2 = -f(r)dt^2 + f(r)^{-1}dr^2 + r^2 d\Omega^2, \quad \text{where} \quad f(r) = (1 - 2M/r). \tag{2.6}$$

Here, t and r represent the time and radial coordinates respectively, and $d\Omega^2$ denotes the metric on a 2-sphere.

At $r = 2M$, known as the event horizon of the black hole [1], the metric component g_{00} tends to zero, and g_{rr} diverges, indicating an apparent singularity. In order to find whether this singularity is physical or simply coordinate-related, let us follow the same procedure we took with the Rindler metric: write the metric in affine null coordinates and observe if it is analytic and non-vanishing at the event horizon.

2.2.1 Metric near $r = 2M$

The metric for $r > 2M$ can be written as

$$ds^2 = f(r)\left[-dt^2 + dr_*^2\right] + r^2 d\Omega^2 = f(r)\left[-du\, dv\right] + r^2 d\Omega^2, \tag{2.7}$$

where $u, v \in (-\infty, \infty)$ are null coordinates defined as in (2.3), and r_* is a tortoise coordinate defined by $dr_* = dr/f(r)$.

Note that $f(r)$ can be expressed implicitly in terms of the new null coordinates. Although an explicit expression would require inverting r_* and determining $r = r(u, v)$, given that we are mainly interested in finding affine coordinates near the event horizon at $r = 2M$, we can perform a local inversion allowed by the implicit function theorem: for r sufficiently close to $2M$ (but larger), we straightforwardly obtain $f(r) = 1 - \frac{2M}{r} \approx e^{-1}e^{(v-u)/4M}$, which leads to the following metric close to $r = 2M$:

$$ds^2 \approx e^{-1}e^{(v-u)/4M}(-du\, dv) + r^2 d\Omega^2 = -e^{-1}dU\, dV + r^2 d\Omega^2, \tag{2.8}$$

where we have defined the Kruskal coordinates:

$$U = -4Me^{-u/4M}, \quad V = 4Me^{v/4M}. \tag{2.9}$$

with $U \in (-\infty, 0)$ and $V \in (0, \infty)$.

The sector $\{t, r\}$ in (2.8) resembles closely what we encountered in the sector $\{t, x\}$ of the maximal analytic extension (2.4) of Rindler spacetime in 1+1, so the new coordinates U and V can be extended to range from $-\infty$ to ∞. From this, we conclude that the coordinates U and V are locally affine near $r = 2M$ where they present no physical problems, confirming that the apparent singularity at the event horizon—i.e., $U = 0$ or $V = 0$—is a coordinate singularity, and can therefore be crossed without encountering a physical obstruction.

It can be shown [4] that, when written in terms of the extended variables U and V, the Schwarzschild metric in the exterior region ($r > 2M$) takes the form

$$ds^2 = -\frac{2M}{r}e^{-r/2M}dU\, dV + r^2 d\Omega^2, \tag{2.10}$$

where $r = r(U, V)$ is implicitly defined by the equation

$$UV = -2Me^{r/2M}(r - 2M). \tag{2.11}$$

From (2.10) and (2.11), the following expression of t in terms of U, V can be obtained:

$$2M \log|V/U| = t. \tag{2.12}$$

It is especially important to note here that the coordinate chart $\{t, r\}$ breaks down at the event horizon $r = 2M$ and therefore fail to describe the region inside the black hole ($r < 2M$). To address this, new coordinates can be defined via (2.11) and (2.12) which we will continue to denote as $\{t, r\}$ for simplicity, despite being entirely unrelated to the coordinate chart describing the exterior region. In fact, this difference is so significant that one can show [1, 10] that for $r < 2M$ the Schwarzschild time t becomes spacelike and the radial coordinate r becomes timelike.

2.2.2 Metric near $r = 0$

As discussed before, the metric becomes ill-defined at $r = 0$. To determine whether this singularity is physical or coordinate-related, one could follow the same procedure used to analyze the apparent singularity at $r = 2M$. However, a quicker method involves evaluating a non-null, curvature-invariant scalar such as the Kretschmann in this region. Upon computing $R_{\mu\nu\rho\sigma}R^{\mu\nu\rho\sigma}$, it is found to diverge, which provides a conclusive indication that the metric is singular at $r = 0$, leading to what is known as 'geodesic incompleteness' [11].

2.2.3 Penrose diagram for Schwarzschild spacetime

In order to understand the causal structure of Schwarzschild spacetime, it is useful to represent its Penrose diagram by means of a conformal compactification [4]. Penrose diagrams help us see the global causal structure in a more clear, compact way: it allows mapping and rescaling the entire spacetime into a finite diagram where horizons are null boundaries, infinities are compacted into finite points, and the singularity is an unavoidable endpoint for infalling observers.

Starting from the Kruskal coordinates (U, V) defined in (2.9), we perform the following coordinate transformation:

$$U = 4M \tan \tilde{U}, \quad V = 4M \tan \tilde{V}. \tag{2.13}$$

This compacts the infinite range of U and V into finite intervals $\tilde{U}, \tilde{V} \in (-\pi/2, \pi/2)$, allowing us to construct a finite diagram—denoted as Penrose diagram—whose boundaries correspond to singularities ($r = 0$) and asymptotic regions ($r, t \to \pm\infty$). The Penrose diagram, presented in Fig. 1, consists of four regions separated by null horizons $\tilde{U} = 0$ (future horizon $\mathcal{H}^+$) and $\tilde{V} = 0$ (past horizon $\mathcal{H}^-$). On the one hand, Regions I and III are asymptotically flat regions corresponding to the universe outside of the black hole's event horizon. They contain the future and past null infinities ($\mathcal{I}^+$ and $\mathcal{I}^-$, respectively), which are endpoints of outgoing and incoming null geodesics—i.e., light rays; and also contain a past timelike infinity i_R^-—origin of timelike trajectories—, a spacelike infinity i_R^0—endpoint of spacelike curves—and a future timelike infinity i_R^+—endpoint of timelike geodesics. On the other hand, Region II is the interior region of the black hole, where all timelike and lightlike trajectories end at the spacelike singularity $r = 0$. Region III is the white hole interior region, time-reversed to Region II, where all causal trajectories emerge from the white hole singularity at $r = 0$ and exit into Regions I and IV.

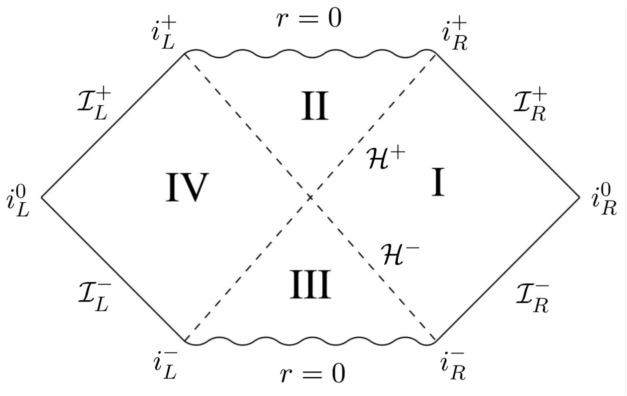

Figure 1: Penrose diagram of the Schwarzschild black hole. Note that regions I and IV are symmetric, and are labeled with a subindex R (right) and L (left), respectively. Adapted from [4].

2.3 Reissner-Nordström metric

The Reissner-Nordström (RN) metric provides a static solution to the Einstein-Maxwell field equations, representing the gravitational field of a charged, non-rotating, spherically symmetric black hole with mass M and charge Q. The metric is given by

$$ds^2 = -f(r)dt^2 + f(r)^{-1}dr^2 + r^2 d\Omega^2, \quad \text{where} \quad f(r) = 1 - \frac{2M}{r} + \frac{Q^2}{r^2}, \tag{2.14}$$

This metric exhibits singularities at $r = 0$ and when $f(r) = 0$. The singularity at $r = 0$ is a true physical singularity, as in the Schwarzschild case, confirmed by the divergence of the curvature invariant $R_{\mu\nu\rho\sigma}R^{\mu\nu\rho\sigma}$. On the other hand, for $f(r) = 0$, solving the quadratic equation for r yields

$$r_\pm = M \pm \sqrt{M^2 - Q^2}. \tag{2.15}$$

Depending on the relationship between M and $|Q|$, there can be two, one, or no real solutions [12]:

a) When $M > |Q|$, known as the physical stable scenario, two coordinate singularities arise, resulting in a black hole with two horizons: one interior and one exterior.

b) When $M = |Q|$, called the extremal case, there is only a single horizon located at $r = M$. This extremal black hole is unstable, since any addition of mass would shift the system back to the standard case where $M > |Q|$.

c) When $M < |Q|$, there are no event horizons. However, the singularity at $r = 0$ persists, meaning it is visible to distant observers without the presence of an event horizon to conceal it. A singularity exposed in this way is referred to as a 'naked singularity'.

Let us consider the case $M > |Q|$. In the following sections, we explore coordinate transformations that allow for the maximal analytical extension of the RN spacetime, removing coordinate singularities as in the Schwarzschild metric.

2.3.1 Maximal extension of the Reissner-Nordström black hole

Noticing that we can rewrite $f(r) = \frac{1}{r^2}(r - r_+)(r - r_-)$, it is easy to observe that this is analogous to the Schwarzschild case but with two horizons instead of just one. It then seems natural to follow the same procedure to reach the maximal analytical extension. Let us consider first the exterior region of the black hole ($r > r_+$): we start rewriting the metric as

$$ds^2 = f(r)\left[-dt^2 + dr_*^2\right] + r^2 d\Omega^2 = f(r)\left[-du\, dv\right] + r^2 d\Omega^2, \tag{2.16}$$

where $u, v \in (-\infty, \infty)$ are null coordinates defined as in (2.3), and r_* is a tortoise coordinate defined by $dr_* = dr/f(r)$.

As done with the Schwarzschild event horizon, let us introduce the Kruskal coordinates:

$$U^+ = -\kappa_+^{-1} e^{-\kappa_+ u}, \quad V^+ = \kappa_+^{-1} e^{\kappa_+ v}, \tag{2.17}$$

where $\kappa_+ = (r_+ - r_-)/2r_+^2$. In terms of these coordinates, the metric becomes

$$ds^2 = -r_+ r_- \frac{e^{-2\kappa_+ r}}{r^2}\left(\frac{r_- - r}{r_-}\right)^{1-\frac{\kappa_+}{\kappa_-}} dU^+\, dV^+ + r^2 d\Omega^2, \tag{2.18}$$

where r is defined implicitly by

$$U^+ V^+ = -\frac{1}{\kappa_+^2} e^{2\kappa_+ r}\left(\frac{r_+ - r}{r_+}\right)\left(\frac{r_- - r}{r_-}\right)^{\frac{\kappa_+}{\kappa_-}}. \tag{2.19}$$

The metric defined in these U^+, V^+ coordinates is regular at the event horizon $r = r_+$, and their ranges can therefore be extended. However, unlike the Schwarzschild case, these extended coordinates do not cover the entire spacetime manifold. To visualize this, let us take a look at the Penrose diagram on the left of Fig. 2: Region I ($r > r_+$) is an asymptotically flat region, with

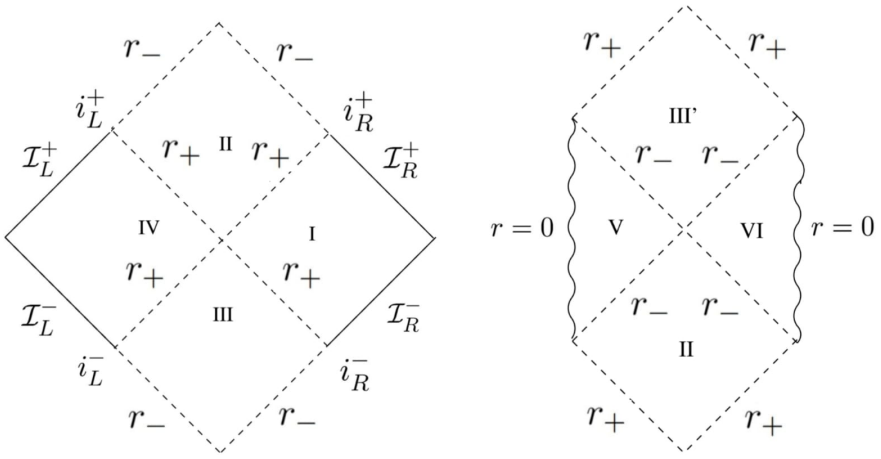

Figure 2: Penrose diagram of the RN black hole corresponding to the Kruskal coordinates U^+, V^+ (left) and U^-, V^- (right). Adapted from [4].

$U^+ = 0$ and $V^+ = 0$ denoting the future and past event horizons, respectively; while region II describes the interior region $r < r_+$ up to $r = r_-$, where the metric becomes singular again.

Therefore, U^+ and V^+ describe the solution in the region $r > r_-$ up to $r = r_-$, another coordinate singularity that can be removed by defining new Kruskal coordinates as follows:

$$U^- = -\kappa_-^{-1} e^{-\kappa_- u}, \quad V^- = \kappa_-^{-1} e^{\kappa_- v}, \tag{2.20}$$

where $\kappa_- = (r_- - r_+)/2r_-^2$. The metric in these new coordinates takes the form

$$ds^2 = -r_+ r_- \frac{e^{-2\kappa_- r}}{r^2} \left(\frac{r_- - r}{r_-}\right)^{1-\frac{\kappa_-}{\kappa_+}} dU^- \, dV^- + r^2 d\Omega^2, \tag{2.21}$$

where r is now defined implicitly by

$$U^- V^- = -\frac{1}{\kappa_-^2} e^{2\kappa_- r} \left(\frac{r_- - r}{r_-}\right) \left(\frac{r_+ - r}{r_+}\right)^{\frac{\kappa_+}{\kappa_-}}. \tag{2.22}$$

In these new coordinates, the metric is regular at $r = r_-$ but singular at $r = r_+$, and thus covers the region $r < r_+$. Focusing now on the Penrose diagram to the right of Fig. 2—which is a continuation of the left diagram—we observe that regions V and VI, corresponding to $0 < r < r_-$, are unique to the RN metric and do not appear in the Schwarzschild solution. In the Schwarzschild case, $r = 0$ is a space-like singularity since g_{tt} changes sign inside the event horizon, but in the RN metric, the true singularity $r = 0$ lies in the region $r < r_-$ where $g_{tt} > 0$, making it a time-like singularity. With time-like singularities, the metric can be extended to future regions, as in region III', encountering another singularity at $r = r_+$, where we can again extend the solution using the Kruskal U^+ and V^+ coordinates. Indeed, comparing both Penrose diagrams in Fig. 2, it is easy to see that they share a common region: $r_- < r < r_+$. Thanks to this overlap, we are capable of constructing the maximal extension of the RN spacetime by patching these regions together infinitely in both the future and the past [4].

3 Canonical Quantization of Charged Fields

In this section, we study the canonical quantization of a charged scalar field in a generic, curved and electromagnetic background, introducing the Klein-Gordon (KG) product and the one-particle and -antiparticle Hilbert spaces. We focus on the ambiguities in defining the quantum vacuum state that result from the different quantization schemes, and compare them using Bogoliubov transformations.

3.1 Classical Field Theory

Let ϕ be a complex scalar field with mass m and charge q, which is propagating in a globally hyperbolic spacetime and satisfies the so-called Klein-Gordon equation:

$$\left(D^\mu D_\mu - m^2\right)\phi = 0, \tag{3.1}$$

where $D_\mu = \nabla_\mu - iqA_\mu$ is the covariant derivative, A_μ is the electromagnetic four-vector potential, and q is the charge of the scalar field. This equation of motion for the field can be obtained applying the principle of least action to the action constructed with the following Lagrangian:

$$\mathcal{L} = -\left[(D^\mu\phi)^*(D_\mu\phi) + m^2\phi^*\phi\right]\sqrt{-\mathfrak{g}}, \tag{3.2}$$

where $\mathfrak{g}$ is the determinant of the metric tensor $g_{\mu\nu}$.

Given that the spacetime is globally hyperbolic, it admits a global time function t [6] and can be decomposed into Cauchy hypersurfaces Σ_t defined by points with constant values of t. Then, the conjugate momentum field corresponding to the scalar field ϕ can be defined by

$$\pi \coloneqq \frac{\partial\mathcal{L}}{\partial(\partial_t\phi)}. \tag{3.3}$$

The only non-vanishing Poisson brackets between the field and its corresponding conjugate momentum are

$$\{\phi(t,\vec{x}), \pi(t,\vec{y})\} = \delta(\vec{x}-\vec{y}), \tag{3.4}$$

where δ denotes the Dirac delta distribution, and $\vec{x}$ and $\vec{y}$ are points in Σ_t, which are independent of the hypersurface Σ_t in which they are calculated [6].

3.1.1 The KG product

In quantum field theory, it is useful to define an inner product between two field solutions, especially when we want to discuss orthogonality and normalization of fields. For scalar fields obeying the KG equation (3.1), such a product is known as the KG product: for any two solutions ϕ_1 and ϕ_2 of the KG equation (3.1), the KG product is defined on a hypersurface Σ_t as:

$$(\phi_1,\phi_2)_{\mathrm{KG}} = -i\int_{\Sigma_t}[\phi_1^* D_\mu\phi_2 - (D_\mu\phi_1)^*\phi_2]d\Sigma^\mu, \tag{3.5}$$

where $d\Sigma^\mu = n^\mu\sqrt{\mathfrak{h}}\,d^3x$ is the surface element, n^μ is a normal unit vector to the Cauchy surface Σ, and $\mathfrak{h}$ is the determinant of the induced metric $h_{\mu\nu} = g_{\mu\nu} + n_\nu n_\nu$—which projects the full 4-dimensional spacetime metric $g_{\mu\nu}$ onto the 3-dimensional surface Σ.

Provided the fields vanish at spatial infinity, the KG product is conserved under time evolution [6]. Besides, it behaves almost like a regular inner product, except it is not positive definite. This means that fields can have a null or even negative 'norm' under this product, which makes it unsuitable as a proper inner product, but allows us still to talk about orthogonality between KG field solutions.

3.1.2 Splittings into positive and negative frequency modes

Let us begin with an orthonormal set of classical mode solutions $\{\phi_n\}$—labeled by a general index n—to the KG equation (3.1), defined with respect to the KG product (3.5). It can be proven [6, 13] that the space of solutions to the KG equation can be split into two complementary subspaces: one which will generate the so-called one-particle Hilbert space (modes that we will call particles) denoted by $\{\phi_n^+\}$ with positive KG norm, and the other which will generate the one-antiparticle Hilbert space (modes that we will call antiparticles) denoted by $\{\phi_n^-\}$ with negative KG norm. This splitting into what is known as 'positive' and 'negative' modes is not arbitrary but due to the fact that the KG product (3.5) is not positive definite. These modes satisfy:

$$(\phi_n^+, \phi_m^+)_{\mathrm{KG}} = -(\phi_n^-, \phi_m^-)_{\mathrm{KG}} = \delta_{mn}, \quad \text{and} \quad (\phi_n^+, \phi_m^-)_{\mathrm{KG}} = 0, \tag{3.6}$$

where the labels n and m can be discrete or continuous, for which all the equations would be written in terms of summations or integrals, and with Kronecker or Dirac deltas, respectively.

Then, any classical solution ϕ can be written as a linear combination of positive and negative modes:

$$\phi = \sum_n (a_n \phi_n^+ + b_n^* \phi_n^-), \tag{3.7}$$

where the sum is taken over the complete basis of modes, and a_n and b_n^* are complex coefficients that can be determined by means of the KG product (3.5):

$$a_n = (\phi_n^+, \phi)_{\mathrm{KG}}, \quad b_n^* = (\phi_n^-, \phi)_{\mathrm{KG}}. \tag{3.8}$$

From (3.4), the only non-vanishing Poisson brackets of these coefficients can be readily obtained:

$$\{a_n, a_m^*\} = \{b_n, b_m^*\} = -i\delta_{nm}. \tag{3.9}$$

3.2 Quantum Field Theory

So far, we have simply required ϕ to be a complex scalar field satisfying the KG equation (3.1), and everything else has followed naturally from it. However, when performing the canonical quantization of the field, a key choice is made: the linear coefficients defining the mode expansion (3.7) are promoted to quantum operators acting on a given Hilbert space.

In this way, a_n and b_n are promoted to annihilation operators $\hat{a}_n$ and $\hat{b}_n$, while their complex conjugates to creation operators $\hat{a}_n^\dagger$ and $\hat{b}_n^\dagger$, all of them acting on a given Fock space, $\mathcal{F}$. The commutation relations for these operators are obtained from the Poisson brackets (3.9) by the usual 'recipe': $\{\cdot,\cdot\} \to [\hat{\cdot},\hat{\cdot}] = i\widehat{\{\cdot,\cdot\}}$, obtaining the following non-zero commutators:

$$[\hat{a}_n, \hat{a}_m^\dagger] = [\hat{b}_n, \hat{b}_m^\dagger] = \delta_{nm}. \tag{3.10}$$

The quantum field operator $\hat{\phi}$ acting on such a Fock state can then be defined as

$$\hat{\phi} = \sum_n (\hat{a}_n \phi_n^+ + \hat{b}_n^\dagger \phi_n^-). \tag{3.11}$$

Given the complex nature of the scalar field and the splitting into positive and negative KG norm modes, we have different operators for particles and antiparticles: $\hat{a}_n$ and $\hat{a}_n^\dagger$ annihilate and create particles, while $\hat{b}_n$ and $\hat{b}_n^\dagger$ do the same for antiparticles.

Finally, the quantum vacuum state $|0\rangle$ is defined as the state devoid of particles or antiparticles—or, in other words, the state annihilated by all the annihilation operators:

$$\hat{a}_n |0\rangle = \hat{b}_n |0\rangle = 0. \tag{3.12}$$

3.3 Quantum vacuum ambiguities

There exists an inherent ambiguity in the definition of our one-particle and -antiparticle Hilbert spaces: different choices of basis of KG field solutions determine different linear coefficients in the mode expansion (3.7) of the scalar field ϕ, leading to different annihilation and creation operators and, consequently, different Fock spaces and quantization schemes, each with its own notion of quantum vacuum, particles and antiparticles [14]. One possible way to compare different quantization schemes is by means of Bogoliubov transformations [5]. In this section, we present this formalism for the general case, and illustrate how different quantizations schemes can be related.

3.3.1 Bogoliubov Transformations

Suppose that, in the process of the canonical quantization of the field ϕ, we choose two distinct orthonormal bases of KG solutions with respect to the KG product (3.5), denoted by $\{\phi_m^{\pm(A)}\}$ and $\{\phi_n^{\pm(B)}\}$. Since both sets form complete bases of the solution space, we can express one set as a linear combination of the other:

$$\phi_n^{+(B)} = \sum_m \left(\alpha_{nm}^{+}\phi_m^{+(A)} + \beta_{nm}^{+}\phi_m^{-(A)}\right), \quad \phi_n^{-(B)} = \sum_m \left(\beta_{nm}^{-}\phi_m^{+(A)} + \alpha_{nm}^{-}\phi_m^{-(A)}\right). \tag{3.13}$$

This change of basis is known as a Bogoliubov transformation, and the coefficients $\alpha_{nm}^{\pm}$ and $\beta_{nm}^{\pm}$ are called Bogoliubov coefficients. These transformations reveal that the β-coefficients quantify the mixing between positive and negative KG norm modes from different bases of solutions. As we will see in Section 4.3, non-zero β-coefficients imply that the the notions of particles and antiparticles might differ from one quantization scheme to another [13]. This mixing is essential for understanding phenomena such as quantum superradiance, and highlights the deep implications that the choice of mode splitting has on the definition of vacuum states and the physical interpretation of particles [13].

Making use of the KG product (3.5) and the orthonormality conditions (3.6), the Bogoliubov coefficients can be written explicitly as

$$\alpha_{nm}^{\pm} = \pm(\phi_m^{\pm(A)}, \phi_n^{\pm(B)})_{\mathrm{KG}}, \quad \beta_{nm}^{\pm} = \mp(\phi_m^{\mp(A)}, \phi_n^{\pm(B)})_{\mathrm{KG}}. \tag{3.14}$$

The classical KG field ϕ can be expanded in terms of either of the two mode sets. Introducing the corresponding creation and annihilation operators $a_m^{(A)}, b_m^{(A)*}$ and $a_n^{(B)}, b_n^{(B)*}$, the field takes the form

$$\phi = \sum_m \left(a_m^{(A)}\phi_m^{+(A)} + b_m^{(A)*}\phi_m^{-(A)}\right) = \sum_n \left(a_n^{(B)}\phi_n^{+(B)} + b_n^{(B)*}\phi_n^{-(B)}\right). \tag{3.15}$$

From this expansion, we can directly obtain the transformation rules between the annihilation and creation operators:

$$a_m^{(A)} = \sum_n \left[\alpha_{nm}^{+}a_n^{(B)} + \beta_{nm}^{-}b_n^{(B)*}\right], \quad b_m^{(A)*} = \sum_n \left[\beta_{nm}^{+}a_n^{(B)} + \alpha_{nm}^{-}b_n^{(B)*}\right]. \tag{3.16}$$

3.3.2 Comparison between different quantizations

The quantum version of these Bogoliubov transformations can be obtained as usual by promoting the linear coefficients of both mode expansions to creation and annihilation operators. However, their respective Fock spaces are not necessarily the same. For clarity, let us name these quantization schemes as the A- and B-quantizations, each associated respectively with vacuum states $|0^{(A)}\rangle$ and $|0^{(B)}\rangle$.

An interesting result arises when computing the expectation value of the number operator $\hat{N}_m^{(A)}$—the number of A-particle and A-antiparticle states from mode m—in the B-vacuum state:

$$\begin{aligned}\langle 0^{(B)}|\,\hat{N}_m^{(A)}\,|0^{(B)}\rangle &= \langle 0^{(B)}|\,\hat{a}_m^{(A)\dagger}\hat{a}_m^{(A)} + \hat{b}_m^{(A)\dagger}\hat{b}_m^{(A)}\,|0^{(B)}\rangle \\ &= \sum_n \langle 0^{(B)}|\left((\alpha_{nm}^+)^*\hat{a}_n^{(B)\dagger} + (\beta_{nm}^-)^*\hat{b}_n^{(B)}\right)\left(\alpha_{nm}^+\hat{a}_n^{(B)} + \beta_{nm}^-\hat{b}_n^{(B)\dagger}\right) \\ &\quad + \left(\beta_{nm}^+\hat{a}_n^{(B)} + \alpha_{nm}^-\hat{b}_n^{(B)\dagger}\right)\left((\beta_{nm}^+)\hat{a}_n^{(B)\dagger} + (\alpha_{nm}^-)^*\hat{b}_n^{(B)}\right)|0^{(B)}\rangle \\ &= \sum_n \left(|\beta_{nm}^-|^2 + |\beta_{nm}^+|^2\right),\end{aligned} \tag{3.17}$$

where we have used the quantum operator transformations analog to (3.16), the commutation relations (3.10), and the definition of quantum vacuum (3.12). Summing over the basis of mode solutions $\{\phi_m^{(A)}\}$, we find that the total number of A-particle/antiparticle states that are present in the B-vacuum state is

$$\mathcal{N} = \sum_m \langle 0^{(B)}|\,\hat{N}_m^{(A)}\,|0^{(B)}\rangle = \sum_{n,m}\left(|\beta_{nm}^-|^2 + |\beta_{nm}^+|^2\right), \tag{3.18}$$

which is not necessarily zero. This result suggests that, in order for the two vacua to coincide, all β-coefficients must vanish—or, in other words, that the splitting of mode solutions must be the same.

4 Charge superradiance

Superradiance refers to a classical effect in which low frequency modes of an incident field are amplified after being scattered off a black hole. Although this phenomenon was first studied for classical fields propagating on a rotating (Kerr) black hole spacetime [15, 16], an analogous effect can also manifest on static, non-rotating, charged black holes, receiving the name of 'charge superradiance' [17].

In this section, we begin with classical superradiance by examining the classical charged scalar modes in the superradiant regime, followed by the canonical quantization of these fields and how they exhibit the quantum counterpart of 'charge superradiance' in the superradiant regime through Bogoliubov transformations.

4.1 Classical superradiance

To study superradiance, we will restrict our attention to Region I of the RN spacetime, presented in Section 2.3. The RN metric is a solution to Einstein's equations with an electromagnetic field, whose 4-vector potential is taken to be

$$A_\mu = (A_0, 0, 0, 0), \quad \text{with} \quad A_0 = -\frac{Q}{r}. \tag{4.1}$$

This particular gauge choice simplifies the expression for the electric field in this region: a black hole with electrical charge Q produces a Coulomb potential in its exterior.

Let now ϕ be a massless, complex scalar field satisfying the massless KG equation of motion (3.1). The choice of a massless scalar field is motivated for two reasons: first, because it simplifies our analysis; and second, because we expect the massless case to already capture the key qualitative features of superradiance that would also appear in the massive case. In support of

this, consider the Schwinger effect—a well-known example of a particle-antiparticle pair creation induced by a background field. It can be shown that, in a static, flat and electromagnetic background similar to the one considered here, the effect is exponentially suppressed for massive fields as $\exp\left[-(Cm^2)/(qE)\right]$, where C is a constant, m and q are the mass and charge of the scalar field, and E is the electric field strength [18]. This suppression suggests that the massless case would dominate in other particle creation processes such as charge superradiance, as we will see.

Due to the spherical symmetry and time-independence of the equation of motion (3.1), a separable solution of this form can be assumed:

$$\phi_{\omega lm}(r) = \mathcal{N}_\omega e^{-i\omega t}\frac{X_{\omega lm}(r)}{r}Y_{lm}(\theta,\varphi), \tag{4.2}$$

where the integer $l = 0, 1, 2\ldots$ is the total angular momentum quantum number, $m = -l, \ldots, l$ is the azimuthal angular momentum quantum number, ω the frequency of the mode, $\mathcal{N}_\omega$ a normalization constant, and $Y_{lm}(\theta,\varphi)$ a spherical harmonic.

Substituting (4.2) into the equation of motion (3.1) yields the radial equation for $X_{\omega l}(r)$:

$$\left[-\frac{d^2}{dr_*^2} + V_{\text{eff}}(r)\right] X_{\omega l}(r) = 0, \tag{4.3}$$

where the effective potential is given by

$$V_{\text{eff}}(r) = \frac{f(r)}{r^2}\left[l(l+1) + rf'(r)\right] - \left(\omega - \frac{qQ}{r}\right)^2. \tag{4.4}$$

In the exterior region of the RN black hole ($r > r_+$), the effective potential takes the following asymptotic values:

$$V_{\text{eff}}(r) \sim \begin{cases} -\widetilde{\omega}^2 = -\left(\omega - \frac{qQ}{r_+}\right)^2, & r_* \to -\infty, \\ -\omega^2, & r_* \to +\infty, \end{cases} \tag{4.5}$$

where $\widetilde{\omega}$ is defined as

$$\widetilde{\omega} = \omega - qQ/r_+. \tag{4.6}$$

Given that the asymptotic values of the effective potential $V_{\text{eff}}(r)$ are constant, the asymptotic forms of the radial part of the solution, $X_{\omega l}(r)$, take the form of plane waves:

$$X(r) \sim \begin{cases} Ce^{i\widetilde{\omega}r_*} + De^{-i\widetilde{\omega}r_*}, & r_* \to -\infty, \\ Ae^{i\omega r_*} + Be^{-i\omega r_*}, & r_* \to +\infty, \end{cases} \tag{4.7}$$

where the coefficients A, B, C, D are complex coefficients to be determined by boundary conditions.

In region I of the Penrose diagram for the RN black hole (see Fig. 2), a complete basis of solutions to equation (3.1) can be constructed by imposing specific boundary conditions on different Cauchy surfaces. For example, let us take boundary conditions that correspond to waves incoming from either past null infinity $\mathcal{I}^-$ or the past horizon $\mathcal{H}^-$, and define two sets of mode solutions: the so-called 'in' and 'up' modes.

To construct the 'in' modes, consider solutions that describe waves incoming from $\mathcal{I}^-$. On a Cauchy surface extending to $\mathcal{H}^- \cup \mathcal{I}^-$—the asymptotic past—we impose the initial condition that

there is only a unit flux coming from $\mathcal{I}^-$ and none from $\mathcal{H}^-$—that is, we set $B^{\rm in} = 1$ and $C^{\rm in} = 0$ in equation (4.7)). The resulting mode $X^{\rm in}_{\omega l}(r)$ describes a wave that is partially reflected back to $\mathcal{I}^+$ (with reflection coefficient $r^{\rm in}_{\omega l}$) and partially transmitted through the future horizon $\mathcal{H}^+$ (with transmission coefficient $t^{\rm in}_{\omega l}$). Its asymptotic behaviour is given by:

$$X^{\rm in}_{\omega l}(r) = \begin{cases} t^{\rm in}_{\omega l}\, e^{-i\widetilde{\omega} r_*}, & r_* \to -\infty, \\ r^{\rm in}_{\omega l}\, e^{-i\omega r_*} + e^{i\omega r_*}, & r_* \to +\infty, \end{cases} \quad \Rightarrow \quad \phi^{\rm in}_{\omega l m} = \mathcal{N}_\omega e^{-i\omega t} \frac{X^{\rm in}_{\omega l}(r)}{r} Y_{ml}(\theta, \varphi). \tag{4.8a}$$

Similarly, the 'up' modes are constructed by imposing initial conditions such that there is only a unit flux coming from the past horizon $\mathcal{H}^-$, with no contribution from $\mathcal{I}^-$—i.e., $C^{\rm up} = 1$ and $B^{\rm up} = 0$ in equation (4.7)). The resulting mode $X^{\rm up}_{\omega l}(r)$ describes a wave partially reflected back to the future horizon $\mathcal{H}^+$ (with coefficient $r^{\rm up}_{\omega l}$) and partly transmitted to $\mathcal{I}^+$ (with coefficient $t^{\rm up}_{\omega l}$). Its corresponding asymptotic form is:

$$X^{\rm up}_{\omega l}(r) = \begin{cases} e^{i\widetilde{\omega} r_*} + r^{\rm up}_{\omega l}\, e^{-i\widetilde{\omega} r_*}, & r_* \to -\infty, \\ t^{\rm up}_{\omega l}\, e^{i\omega r_*}, & r_* \to +\infty, \end{cases} \quad \Rightarrow \quad \phi^{\rm up}_{\omega l m} = \mathcal{N}_\omega e^{-i\omega t} \frac{X^{\rm up}_{\omega l}(r)}{r} Y_{ml}(\theta, \varphi). \tag{4.8b}$$

These two sets of solution modes $\{\phi^{\rm in}_{\omega lm}, \phi^{\rm up}_{\omega lm}\}$ form a complete basis of mode solutions to equation (3.1) that describe the massless scalar field incoming from the asymptotic past in Region I of the RN black hole spacetime.

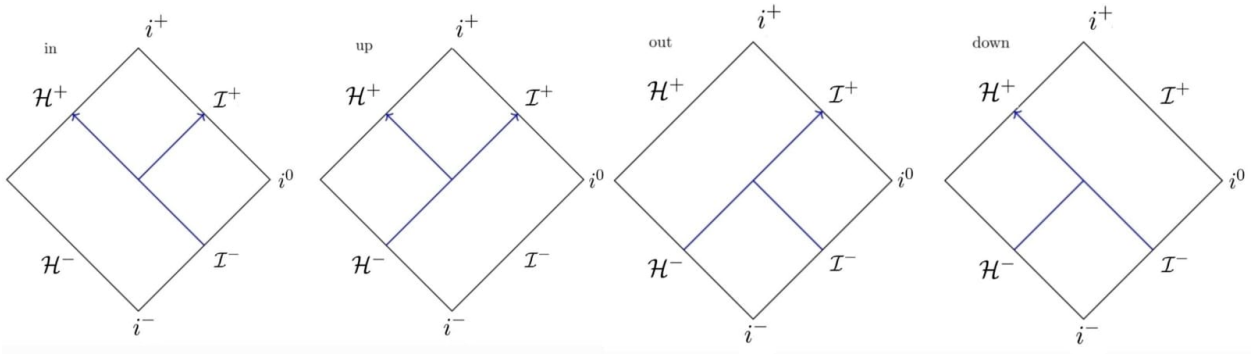

Figure 3: Illustrative summary of inital conditions used to construct the 'in', 'up', 'out', and 'down' modes in region I of the RN spacetime. Adapted from [19].

An alternative complete basis of solutions in Region I is given by the so-called 'out' and 'down' modes, $\{\phi^{\rm out}_{\omega lm}, \phi^{\rm down}_{\omega lm}\}$. These modes are associated with the propagation of the scalar field in the asymptotic future: the 'out' modes correspond to waves emerging at future null infinity $\mathcal{I}^+$, while the 'down' modes correspond to waves entering the future horizon $\mathcal{H}^+$. They can be constructed by following the *reverse* path used to define the 'in' and 'up' mode—this is, by imposing unit fluxes on future Cauchy surfaces rather than past ones. The asymptotic behaviour of these modes are given by:

$$X^{\rm out}_{\omega l}(r) = \begin{cases} t^{\rm out}_{\omega l}\, e^{-i\widetilde{\omega} r_*}, & r_* \to -\infty, \\ e^{-i\omega r_*} + r^{\rm out}_{\omega l}\, e^{i\omega r_*}, & r_* \to +\infty, \end{cases} \quad \Rightarrow \quad \phi^{\rm out}_{\omega lm} = \mathcal{N}_\omega e^{-i\omega t} \frac{X^{\rm out}_{\omega l}(r)}{r} Y_{ml}(\theta, \varphi). \tag{4.9a}$$

$$X^{\rm down}_{\omega l}(r) = \begin{cases} e^{i\widetilde{\omega} r_*} + r^{\rm down}_{\omega l}\, e^{-i\widetilde{\omega} r_*}, & r_* \to -\infty, \\ t^{\rm down}_{\omega l}\, e^{i\omega r_*}, & r_* \to +\infty. \end{cases} \quad \Rightarrow \quad \phi^{\rm down}_{\omega lm} = \mathcal{N}_\omega e^{-i\omega t} \frac{X^{\rm down}_{\omega l}(r)}{r} Y_{ml}(\theta, \varphi). \tag{4.9b}$$

On the other hand, relations between both bases of solutions can be derived using the following Wronskians [20]:

$$X_1 \frac{dX_2}{dr_*} - X_2 \frac{dX_1}{dr_*}, \quad \text{and} \quad X_1^* \frac{dX_2}{dr_*} - X_2 \frac{dX_1^*}{dr_*}, \tag{4.10}$$

which are independent of the r_* at which they are evaluated for any two solutions X_1, X_2 of the radial equation (4.3).

For instance, consider choosing $X_1 = X^{\text{in}}$ and $X_2 = X^{\text{up}}$ in the second Wronskian relation (4.10). Since the Wronskian is independent of r_*, we can evaluate it in two asymptotic regions: near the event horizon ($r_* \to -\infty$) and far from the black hole ($r_* \to \infty$). Matching the results from both limits, we obtain the following relation:

$$\omega t^{\text{up}} r^{\text{in}*} = -\widetilde{\omega} r^{\text{up}} t^{\text{in}*}. \tag{4.11}$$

If we do the same but now with $X_1 = X^{\text{in}}$ and $X_2 = X^{\text{down}}$, we arrive to

$$\omega t^{\text{down}} r^{\text{in}} = -\widetilde{\omega} r^{\text{down}} t^{\text{in}}. \tag{4.12}$$

Given that in the Wronskian relations (4.10) both ω and $\widetilde{\omega}$ can take any real value, we can readily see when comparing both relations that

$$r^{\text{down}} \equiv r^{\text{up}*}, \quad t^{\text{down}} \equiv t^{\text{up}*} \quad \Rightarrow \quad X^{\text{down}} \equiv X^{\text{up}*}. \tag{4.13}$$

Similarly, we can arrive to the relations

$$r^{\text{out}} \equiv r^{\text{in}*}, \quad t^{\text{out}} \equiv t^{\text{in}*} \quad \Rightarrow \quad X^{\text{out}} \equiv X^{\text{in}*}. \tag{4.14}$$

If we continue evaluating the Wronskians relations (4.10) for other combinations of asymptotic radial modes, more relations between the reflection and transmission coefficients of different modes can be derived. From some of these relations, it can be checked that the asymptotic behaviour of the 'out' and 'down' modes can be written as linear combinations of the asymptotic behaviour of the 'in' and 'up' modes as follows:

$$X^{\text{out}}_{\omega l}(r) = r^{\text{in}*}_{\omega l} X^{\text{in}}_{\omega l}(r) + t^{\text{in}*}_{\omega l} X^{\text{up}}_{\omega l}(r), \tag{4.15a}$$

$$X^{\text{down}}_{\omega l}(r) = r^{\text{up}*}_{\omega l} X^{\text{up}}_{\omega l}(r) + t^{\text{up}*}_{\omega l} X^{\text{up}}_{\omega l}(r). \tag{4.15b}$$

Finally, applying the same method with $X_1 = X^{\text{in}}$ and $X_2 = X^{\text{out}}$ (or $X_1 = X^{\text{up}}$ and $X_2 = X^{\text{down}}$) and evaluating their asymptotic form in the Wronskian relations (4.10), we arrive to

$$\omega[1 - |r^{\text{in}}|^2] = \widetilde{\omega}|t^{\text{in}}|^2, \quad \text{and} \quad \widetilde{\omega}[1 - |r^{\text{up}}|^2] = \omega|t^{\text{up}}|^2. \tag{4.16}$$

From any of these two relations, it is straightforward to see that for scalar fields with $\omega\widetilde{\omega} < 0$, the reflection coefficient $|r_{\omega l}|^2 > 1$. This means that when a field is scattered off a black hole, there is more reflected radiation than incident. This phenomenon is denominated classical superradiance, and only occurs for charged scalar fields with frequencies in the so-called 'superradiant regime': $\min\left\{-\frac{qQ}{r_+}, 0\right\} < \omega < \max\left\{0, \frac{qQ}{r_+}\right\}$, which depends on the relative sign between the charges of the black hole and the charged field.

4.2 Normalization of modes

Let us now compute the KG products (3.5) of pairs of 'in' and 'up' modes in a Cauchy's surface close to $\mathcal{H}^- \cup \mathcal{I}^-$—the region where the initial conditions for these modes are defined—, and of two 'out' and 'down' modes in the Cauchy's surface close to $\mathcal{H}^+ \cup \mathcal{I}^+$—where those modes were defined. It can be shown [19] that these products result in:

$$(\phi^{\text{in/out}}_{\omega lm}, \phi^{\text{in/out}}_{\omega' l' m'})_{\text{KG}} = 4\pi\omega \mathcal{N}^{\text{in/out}*}_{\omega} \mathcal{N}^{\text{in/out}}_{\omega'} \delta(\omega - \omega')\delta_{ll'}\delta_{mm'}, \tag{4.17a}$$

$$(\phi^{\text{up/down}}_{\omega lm}, \phi^{\text{up/down}}_{\omega' l' m'})_{\text{KG}} = 4\pi\widetilde{\omega} \mathcal{N}^{\text{up/down}*}_{\omega} \mathcal{N}^{\text{up/down}}_{\omega'} \delta(\omega - \omega')\delta_{ll'}\delta_{mm'}. \tag{4.17b}$$

As one can readily see, modes with different frequency ω or quantum numbers l and m are orthogonal, as are any 'in' mode to any 'up' mode, and any 'out' mode to any 'down' mode.

The frequency-dependent nature of the KG norms of the modes (4.17) will play an essential role during the canonical quantization of the fields. As discussed in Section 3.1.2, the particle and antiparticle interpretations of field modes depend on their KG norm: solutions with positive KG norm correspond to particles, while solutions with negative KG norm correspond to antiparticles. Thus, one can observe that for the 'in' and 'out' modes, particles are associated with $\omega > 0$ and antiparticles with $\widetilde{\omega} < 0$, while for the 'up' and 'down' modes, particles correspond to $\widetilde{\omega} > 0$ and antiparticles to $\widetilde{\omega} < 0$.

4.3 Comparison between the 'in' and 'out' states

We have explored the classical phenomenon of charge superradiance, which is simply a scattering process in which there is more reflected radiation than incident. In this section, we investigate whether there is a purely quantum contribution to this effect outside the event horizon of the black hole. In order to do so, we will construct two quantum vacuum states—by means of the canonical quantization of the scalar field in the RN spacetime—and compare them following the procedure described in Section 3. If we find non-vanishing β-coefficients, it would imply the existence of a quantum phenomenon of creation of particles, and therefore charge superradiance would have a quantum counterpart.

In Section 4.1, we found two bases of solutions to equation (3.1) according to different physical observers in the spacetime of the black hole: $\{\phi^{\text{in}}_{\omega lm}, \phi^{\text{up}}_{\omega lm}\}$ and $\{\phi^{\text{out}}_{\omega lm}, \phi^{\text{down}}_{\omega lm}\}$. These two bases construct different states: the past and future Boulware states—also denoted as the 'in' and 'out' states [8]—respectively.

4.3.1 Past Boulware or 'in' state

Let us construct a past state defined with respect to a Cauchy surface close to $\mathcal{H}^- \cup \mathcal{I}^-$. In this region of spacetime, it is natural to use the Schwarzschild-like coordinate t as the time coordinate.

The past Boulware state can be constructed as usual: first, we choose a basis, which in this case will be the 'in-up' basis $\{\phi^{\text{in}}_{\omega lm}, \phi^{\text{up}}_{\omega lm}\}$, and then split it into positive and negative KG norm modes. However, this splitting is not arbitrary but due to the non-positive-definite nature of the KG product: according to our criterion, particles are associated with modes with positive KG norm, while antiparticles are associated with those with negative KG norm. Thus, knowing how the KG norm of the modes (4.17) depends on either ω or $\widetilde{\omega}$, we can straightforwardly split the 'in' modes into $\{\phi^{\text{in}\pm}_{\omega lm}\}$, where we have defined $\phi^{\text{in}+}_{\omega lm}$ as the modes with positive frequency, $\omega > 0$, and $\phi^{\text{in}-}_{\omega lm}$ as those with negative frequency, $\omega < 0$. For the 'up' modes, a similar splitting is done but now with respect to the sign of $\widetilde{\omega}$ such that they are split into $\{\phi^{\text{up}\pm}_{\omega lm}\}$ with $\phi^{\text{up}+}_{\omega lm}$ defined as the modes with $\widetilde{\omega} > 0$, and $\phi^{\text{up}-}_{\omega lm}$ as those with $\widetilde{\omega} < 0$.

Then, the past quantum scalar field can be expanded in terms of these 'in' and 'up' modes as follows:

$$\hat{\phi}_{|\text{in}\rangle} = \sum_{l,m} \left[\int_0^\infty d\omega\, \hat{a}^{\text{in}}_{\omega lm} \phi^{\text{in}+}_{\omega lm} + \int_{-\infty}^0 d\omega\, \hat{b}^{\text{in}\dagger}_{\omega lm} \phi^{\text{in}-}_{\omega lm} + \int_0^\infty d\widetilde{\omega}\, \hat{a}^{\text{up}}_{\omega lm} \phi^{\text{up}+}_{\omega lm} + \int_{-\infty}^0 d\widetilde{\omega}\, \hat{b}^{\text{up}\dagger}_{\omega lm} \phi^{\text{up}-}_{\omega lm} \right]. \tag{4.18}$$

It is important to note that the operators $\hat{a}^{\text{in}}_{\omega lm}$ and $\hat{b}^{\text{in}}_{\omega lm}$ are defined only for $\omega > 0$ and $\omega < 0$ respectively, while $\hat{a}^{\text{up}}_{\omega lm}$ and $\hat{b}^{\text{up}}_{\omega lm}$ are defined only for $\widetilde{\omega} > 0$ and $\widetilde{\omega} < 0$, respectively. Their Hermitian adjoint counterparts are defined over the same frequency ranges. All these operators satisfy the standard commutation relations given in (3.10).

The past Boulware state, or 'in' vacuum $|\text{in}\rangle$, is defined as in (3.12), that is, it is state annihilated by the annihilation operators $\hat{a}^{\text{in}}_{\omega lm}$, $\hat{b}^{\text{in}}_{\omega lm}$, $\hat{a}^{\text{up}}_{\omega lm}$, and $\hat{b}^{\text{up}}_{\omega lm}$, each within their respective frequency domains. This state represents a vacuum in which no particles or antiparticles are incoming from past null infinity $\mathcal{I}^-$, nor outgoing from the past horizon $\mathcal{H}^-$.

4.3.2 Future Boulware or 'out' state

Analogously to the past Boulware state, the future Boulware state is defined with respect to a Cauchy surface near $\mathcal{H}^+ \cup \mathcal{I}^+$. We now expand the field in terms of the 'out-down' mode basis $\{\phi^{\text{out}}_{\omega lm}, \phi^{\text{down}}_{\omega lm}\}$, instead of the 'in-up' mode basis. In this case, according to (4.17), the sign of the norms of the 'out' and 'down' modes is the same as the sign of ω and $\widetilde{\omega}$, respectively. Therefore, we can split the modes into: $\phi^{\text{out}+}_{\omega lm}$ and $\phi^{\text{down}+}_{\omega lm}$ having $\omega > 0$; and $\phi^{\text{out}-}_{\omega lm}$ and $\phi^{\text{down}-}_{\omega lm}$ having $\widetilde{\omega} < 0$.

The future quantum scalar field can then be expanded in terms of these 'out' and 'down' modes as follows:

$$\hat{\phi}_{|\text{out}\rangle} = \sum_{l,m} \left[\int_0^\infty d\omega\, \hat{a}^{\text{out}}_{\omega lm} \phi^{\text{out}+}_{\omega lm} + \int_{-\infty}^0 d\omega\, \hat{b}^{\text{out}\dagger}_{\omega lm} \phi^{\text{out}-}_{\omega lm} + \int_0^\infty d\widetilde{\omega}\, \hat{a}^{\text{down}}_{\omega lm} \phi^{\text{down}+}_{\omega lm} + \int_{-\infty}^0 d\widetilde{\omega}\, \hat{b}^{\text{down}\dagger}_{\omega lm} \phi^{\text{down}-}_{\omega lm} \right], \tag{4.19}$$

where the annihilation and creation operators are defined for the same range of ω and $\widetilde{\omega}$ as in the past case—identifying the 'out' and 'down' operators with the 'in' and 'up' ones, respectively—and satisfy the same commutation relations (3.10).

The future Boulware state, or 'out' vacuum, $|\text{out}\rangle$, is defined as the state annihilated by the annihilation operators $\hat{a}^{\text{out}}_{\omega lm}$, $\hat{b}^{\text{out}}_{\omega lm}$, $\hat{a}^{\text{down}}_{\omega lm}$, and $\hat{b}^{\text{down}}_{\omega lm}$, as in (3.12). It corresponds to a vacuum with no particles or antiparticles detected at future null infinity $\mathcal{I}^+$ or emerging from the future event horizon $\mathcal{H}^+$.

4.3.3 Mixing of modes

Let us first consider the case $qQ > 0$. After splitting all the mode bases into positive and negative KG norm components accordingly, it can be readily seen from (4.15) that the 'out' and 'down' modes can be expressed as linear combinations of positive and negative KG norm 'in' and 'up' modes:

$$\phi^{\text{out}+}_{\omega lm} = \begin{cases} r^{\text{in}*}_{\omega l}\, \phi^{\text{in}+}_{\omega lm} + t^{\text{in}*}_{\omega l}\, \phi^{\text{up}-}_{\omega lm}, & 0 < \omega < qQ/r_+, \\ r^{\text{in}*}_{\omega l}\, \phi^{\text{in}+}_{\omega lm} + t^{\text{in}*}_{\omega l}\, \phi^{\text{up}+}_{\omega lm}, & \omega > qQ/r_+; \end{cases} \tag{4.20a}$$

$$\phi^{\text{out}-}_{\omega lm} = r^{\text{in}*}_{\omega l}\, \phi^{\text{in}-}_{\omega lm} + t^{\text{in}*}_{\omega l}\, \phi^{\text{up}-}_{\omega lm}, \quad \omega < 0; \tag{4.20b}$$

$$\phi^{\text{down}+}_{\omega lm} = r^{\text{up}*}_{\omega l}\, \phi^{\text{up}+}_{\omega lm} + t^{\text{up}*}_{\omega l}\, \phi^{\text{up}+}_{\omega lm}, \quad \omega > qQ/r_+; \tag{4.20c}$$

$$\phi^{\text{down}-}_{\omega lm} = \begin{cases} r^{\text{up}*}_{\omega l}\, \phi^{\text{up}-}_{\omega lm} + t^{\text{up}*}_{\omega l}\, \phi^{\text{in}+}_{\omega lm}, & 0 < \omega < qQ/r_+, \\ r^{\text{in}*}_{\omega l}\, \phi^{\text{in}+}_{\omega lm} + t^{\text{in}*}_{\omega l}\, \phi^{\text{up}+}_{\omega lm}, & \omega < 0. \end{cases} \tag{4.20d}$$

From these expressions, it is clear that the modes $\phi^{\text{out}-}_{\omega lm}$ and $\phi^{\text{down}+}_{\omega lm}$ are expanded only in terms of negative and positive KG norm modes, respectively. This can easily be checked noticing that, according to (4.6), modes with $\omega < 0$ satisfy $\widetilde{\omega} < 0$, and modes with $\omega > qQ/r_+$ satisfy $\widetilde{\omega} > 0$. Therefore, there is no mixing of positive and negative KG norm modes and, from the general Bogoliubov transformations (3.13), the corresponding β-coefficients of these modes are zero.

However, only in the low frequency range $0 < \omega < qQ/r_+$—which coincides with the classical superradiant regime—it is observed that the modes $\phi^{\text{out}+}_{\omega lm}$ and $\phi^{\text{down}-}_{\omega lm}$ are expanded into a superposition of positive and negative KG norm modes from the 'in-up' basis. Consequently, the β-coefficients associated with these expansions are nonzero in this regime, and—by comparison with (3.13)—can be identified explicitly in terms of the transmission coefficients as follows:

$$\beta^{\text{out}-\text{up}}_{\omega\omega' ll' mm'} = \begin{cases} t^{\text{in}*}_{\omega l}\, \delta(\omega-\omega')\delta_{ll'}\delta_{mm'}, & 0<\omega<qQ/r_+, \\ 0, & \omega > qQ/r_+; \end{cases} \tag{4.21a}$$

$$\beta^{\text{in}-\text{down}}_{\omega\omega' ll' mm'} = \begin{cases} t^{\text{up}*}_{\omega l}\, \delta(\omega-\omega')\delta_{ll'}\delta_{mm'}, & 0<\omega<qQ/r_+, \\ 0, & \omega < 0. \end{cases} \tag{4.21b}$$

We arrive to analogous conclusions for the case $qQ < 0$, with the only difference in that the non-vanishing β-coefficients are now associated to the modes $\phi^{\text{out}-}_{\omega lm}$ and $\phi^{\text{down}+}_{\omega lm}$ in the interval $-|qQ|/r_+ < \omega < 0$.

Now, by taking the 'in' vacuum state and evolving it to the infinite future, we can compute the expectation value of the number operator associated with the 'out' modes. This allows us to determine the total number of particles in the future Boulware state that are perceived in the past Boulware vacuum, which can be expressed as:

$$\begin{aligned} \mathcal{N} &= \sum_n \langle \text{in}|\hat{a}^{\text{out}\dagger}_n \hat{a}^{\text{out}}_n + \hat{a}^{\text{down}\dagger}_n \hat{a}^{\text{down}}_n + \hat{b}^{\text{out}\dagger}_n \hat{b}^{\text{out}}_n + \hat{b}^{\text{down}\dagger}_n \hat{b}^{\text{down}}_n|\text{in}\rangle \\ &= \sum_{n,m} \left(|\beta^{\text{out}-\text{up}}_{nm}|^2 + |\beta^{\text{in}-\text{down}}_{nm}|^2 \right) = 2\sum_{n,m} \left(|t^{\text{out}}_{\omega l}|^2 (\delta(\omega-\omega'))^2 \delta^2_{ll'}\delta^2_{mm'}| \right) \\ &= 2\delta(0) \sum_{l=0}^{\infty} \sum_{m=-l}^{l} \int_{\min\left\{-\frac{qQ}{r_+},0\right\}}^{\max\left\{0,\frac{qQ}{r_+}\right\}} d\omega\, |t^{\text{out}}_{\omega l}|^2, \end{aligned} \tag{4.22}$$

where $n = \omega lm$ and $m = \omega' l' m'$ are labels, and the integration is performed over the superradiant regime. The result is that there is an infinite number of particles due to the term $\delta(0)$ which comes from integrating the square delta function: $(\delta(\omega-\omega'))^2 = \delta(0)\,\delta(\omega-\omega')$. This is no surprise given that we are integrating over all time in a static situation, and therefore we define the total number of particles per unit time instead:

$$\mathcal{N}' = 2\sum_{l=0}^{\infty} \sum_{m=-l}^{l} \int_{\min\left\{-\frac{qQ}{r_+},0\right\}}^{\max\left\{0,\frac{qQ}{r_+}\right\}} d\omega\, |t^{\text{out}}_{\omega l}|^2. \tag{4.23}$$

An explicit expression for the transmission coefficient $t^{\text{out}}_{\omega l}$ can be directly obtained from the asymptotic behaviour of the 'out' radial mode $X^{\text{out}}_{\omega l}$, as given in (4.9a):

$$t^{\text{out}}_{\omega l} = \lim_{r_* \to -\infty} X^{\text{out}}_{\omega l}(r)\, e^{i\widetilde{\omega} r_*}. \tag{4.24}$$

This quantity can be computed numerically by solving the radial equation (4.3) for $X_{\omega l}(r)$ and imposing the boundary conditions used to define the 'out' mode in Section 4.1. Specifically, on a Cauchy's surface near $\mathcal{H}^+ \cup \mathcal{I}^+$, we impose that the solution behaves as $X_{\omega l}(r) \to e^{-i\widetilde{\omega} t}$ close to future null infinity $\mathcal{I}^+$, and vanishes close to the future event horizon $\mathcal{H}^+$, i.e., $X_{\omega l}(r) \to 0$ as $r_* \to -\infty$.

5 Conclusions

In this thesis, we have introduced the framework of semiclassical gravity by quantifying a charged scalar field on classical black hole backgrounds. We then explored how the ambiguity in the choice of vacuum—an intrinsic property of quantum field theory in curved spacetimes—can lead to physical phenomena such as charge superradiance, whose classical and quantum versions were analyzed in a charged black hole background.

We began with the classical description of Rindler, Schwarzschild and Reissner-Nordström spacetimes, analyzing their causal structure using Penrose diagrams and distinguishing between physical singularities—due to the breakdown of spacetime itself—and coordinate ones—due to a bad choice of coordinates—by means of their maximal analytical extensions. This geometric analysis provided a solid foundation for developing the quantum field theory framework that followed.

We then formulated the canonical quantization of a complex scalar field on a fixed, curved and electromagnetic background, introducing the KG inner product and highlighting its role in defining orthogonal mode solutions. We found an inherent ambiguity in defining a vacuum state in curved spacetime, which emerges from how one splits the space of KG solutions into positive and negative KG norm modes—an essential step to construct the Fock space. While in flat spacetime this splitting relies on Poincaré symmetry and leads to a canonical notion of vacuum, no such preferred criterion exists in a generic curved spacetime. As a consequence, each distinct choice of mode decompositions gives rise to a different quantization, each with its own vacuum state and corresponding notion of particle. This observer dependence is captured by Bogoliubov transformations, which relate different quantization schemes and quantify the particle content of one vacuum state with respect to another.

The final part of the thesis was centered in examining the phenomenon of superradiance in RN black holes. At the classical level, we showed that certain low-frequency charged bosonic modes are scattered off the black hole with a reflection coefficient greater than one, an effect denominated charge superradiance. We then constructed the so-called past and future Boulware vacua—quantum states naturally associated with observers near past and future null infinity, respectively—and compared them via Bogoliubov transformations. During this process, we found that the splitting into positive and negative KG norm modes is not arbitrary but fixed due to the not positive definite nature of the KG product (3.5). Finally, we found that, within the superradiant regime, the 'in' and 'out' vacuum states are not equivalent: even in the absence of classical incoming radiation, there exists a non-zero flux of outgoing particles. This highlights the connection between the ambiguity in the vacuum choice and physically observable quantum effects. In particular, if we computed the expectation values of operators such as the scalar current $\hat{J}^\mu$ or the stress-energy tensor $\hat{T}^{\mu\nu}$, we would find that they differ when evaluated in the 'in' versus the 'out' vacuum state [21]. In the same way that we observe a net outgoing particle flux—in a region outside of the black hole event horizon—we also find a non-zero flux of charge and energy emerging from the black hole. Physically, this implies that energy is being extracted from the black hole due to the combined presence of spacetime curvature and an external electric field [19]. This particle creation phenomenon is a purely quantum effect, and it occurs in addition to the classical effect. It is important to note that for quantum charge superradiance, particles are produced spontaneously, without any incoming radiation—unlike for the classical case.

Overall, this thesis provides a self-contained overview of semiclassical methods in black hole physics. A natural continuation would involve numerically computing the transmission coefficients in (4.23) to quantify the particle flux in each mode. It would also be interesting to extend the analysis to fermionic fields, as done in [21], or explore physical states other than the Future and Past Boulware states that can be constructed, such as the Past and Future Unruh states [19].

References

[1] S. M. Carroll, *Spacetime and Geometry: An Introduction to General Relativity*. Addison-Wesley, 2004.

[2] M. Maggiore, *A Modern introduction to quantum field theory*. Oxforx University Press, 2005.

[3] S. W. Hawking, *Particle creation by black holes*, *Commun. Math. Phys.* **43** (1975) 199.

[4] A. Fabbri and J. Navarro-Salas, *Modeling Black Hole Evaporation*. Imperial College Press, 2005.

[5] N. D. Birrell and P. C. W. Davies, *Quantum Fields in Curved Space*. Cambridge University Press, 1982.

[6] L. J. Garay, *Lecture notes: Quantum fields in curved spacetimes*, (2015).

[7] W. G. Unruh, *Notes on black-hole evaporation*, *Physical Review D* **14** (1976) 870.

[8] V. Balakumar, E. Winstanley, R. P. Bernar, and L. C. Crispino, *Quantum superradiance on static black hole space-times*, *Phys. Lett. B* **811** (2020) 135904.

[9] V. Mukhanov and S. Winitzki, *Introduction to Quantum Effects in Gravity*. Cambridge University Press, 2007.

[10] R. M. Wald, *General Relativity*. University of Chicago Press, 1984.

[11] S. W. Hawking and G. F. R. Ellis, *The Large Scale Structure of Space-Time*. Cambridge University Press, 1973.

[12] J. Nordebo, *The reissner-nordström metric*, Master's thesis, Umeå University, (2016).

[13] A. Álvarez-Domínguez, *Canonical quantization of charged fields in the presence of intense electromagnetic fields*. PhD thesis, Universidad Complutense de Madrid, 2025. Under review.

[14] S. A. Fulling, *Nonuniqueness of canonical field quantization in riemannian space-time*, *Phys. Rev. D* **7** (1973) 2850.

[15] R. Brito, V. Cardoso, and P. Pani, *Superradiance: Energy Extraction, Black-Hole Bombs and Instabilities*. Springer, 2015.

[16] W. H. Press and S. A. Teukolsky, *Floating orbits, superradiant scattering and the black-hole bomb*, *Nature* **238** (1972) 211.

[17] J. D. Bekenstein, *Extraction of energy and charge from a black hole*, *Phys. Rev. D* **7** (1973) 949.

[18] J. Schwinger, *On gauge invariance and vacuum polarization*, *Phys. Rev.* **82** (1951) 664.

[19] V. Balakumar, R. P. Bernar, and E. Winstanley, *Quantization of a charged scalar field on a charged black hole background*, *Phys. Rev. D* **106** (2022) 125013.

[20] L. J. Garay, *Lecture Notes: Mathematical Methods I*, (2022).

[21] A. Álvarez-Domínguez and E. Winstanley, *Quantum fermion superradiance and vacuum ambiguities on charged black holes*, *J. High Energy Phys.* **2025** (2025) 118.